ACS Sustainable Chemistry & Engineering

Research Article

pubs.acs.org/journal/ascecg

Hierarchical Carbon Nanotube/Carbon Black Scaffolds as Short- and Long-Range Electron Pathways with Superior Li-Ion Storage Performance

Xin-Yan Liu,[†,⊥] Hong-Jie Peng,[†,⊥] Qiang Zhang,[*,†] Jia-Qi Huang,[†] Xiao-Fei Liu,[†,‡] Li Wang,[§] Xiangming He,[§] Wancheng Zhu,[‡] and Fei Wei[†]

[†]Beijing Key Laboratory of Green Chemical Reaction Engineering and Technology, Department of Chemical Engineering and [§]Institute of Nuclear and New Energy Technology, Tsinghua University, Beijing 100084, P. R. China

[‡]Department of Chemical Engineering, Qufu Normal University, Shandong 273165, P. R. China.

ABSTRACT: The combination of nanocarbon building blocks into hierarchical nanostructures is expected to bring good distribution of each element and even lead to formation of multifunctional composite cathodes with unexpected Li ion storage performance. The strategies toward fully demonstrating the potential of nanocarbon as three-dimensional (3D) conductive scaffolds for cathodes are highly required to broaden the application of nanocarbon in energy storage. Herein, hierarchical carbon nanotube/carbon black (CNT/CB) scaffolds were employed to promote the possible short- and long-range electron pathways in different scales within the $LiFePO_4$ cathode. With the construction of hierarchical CNT/CB conductive scaffolds, the $LiFePO_4$/C cathode exhibits enhanced Li storage performance and improved electrochemical kinetics. At a current density of 0.2 C, $LiFePO_4$/C cathode with such hierarchical CNT/CB networks exhibited reversible discharge capacity of 156.9 mAh g^{-1} over 50 cycles. When the current density was increased to 1.2 C, a capacity of 119.1 mAh g^{-1} was still preserved, and a capacity of 150.5 mAh g^{-1} at 0.2 C rate was available after 1.2 C rate, indicating a high reversibility of the composite cathode. This strategy to hybridize CNTs and CBs into hierarchical scaffolds not only demonstrated its high efficiency to build $LiFePO_4$/C composite cathodes with excellent Li storage performance and good economy but also could be applied to supercapacitors, redox flow batteries, and Li/S and Li/O_2 batteries with improved energy storage performance.

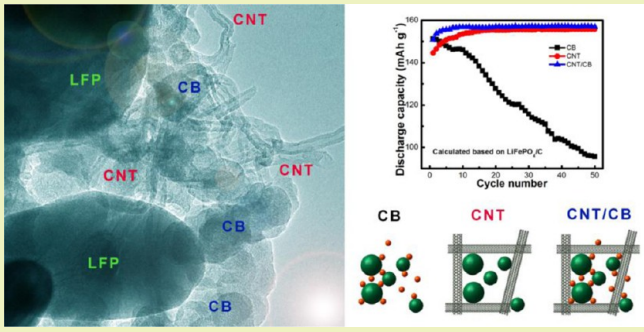

KEYWORDS: *Li-ion battery, Carbon nanotube, $LiFePO_4$, Cathode, Conductive filler, Electron pathway, Hierarchical nanostructure, Energy storage*

INTRODUCTION

Chemical energy storages using rechargeable Li-ion batteries are becoming more and more important to meet the rapidly increasing demands from portable electronic devices, electrical vehicles, hybrid electrical vehicles, and so on.[1] The rapid innovation on the composite electrode provides the driving force for the continuous improvement on the Li storage performance for sustainable society. The cathode materials are typically oxides/phosphates of transition metals, which can undergo oxidation to higher valences when lithium is removed. For instance, olivine-type $LiFePO_4$ have attracted great attention due to a high theoretical specific capacity (ca. 170 mAh g^{-1}) when the Li^+ ions are extracted from $LiFePO_4$ and inserted into $FePO_4$ with a flat plateau of around 3.5 V vs Li/Li^+.[2,3] However, it is very difficult to obtain the full capacity because of the extremely low electronic conductivity of $LiFePO_4$ at ca. 10^{-9} S cm^{-1}, which leads to initial capacity loss and poor rate capability caused by the sluggish diffusion of Li^+ ion in the olivine structure.[4]

Many efficient strategies have been proposed to overcome this drawback, including (1) coating a conductive layer around the insulate cathode particles,[5−7] (2) ionic substitution to enhance the electrochemical properties,[8] (3) synthesis of cathode particles with well-defined morphology,[2,9] and (4) addition of nanocarbon fillers to form three-dimensional (3D) conductive networks in the cathodes.[10] The addition of high conductive carbon blacks (CBs) were widely accepted by Li-ion battery industry.[11]

Recently, with the rise of nanomaterial research, highly conductive nanocarbon materials, such as carbon nanotubes (CNTs),[12−17] vapor grown carbon fibers,[18] graphene,[19−21] and CNT/graphene hybrid,[22,23] have been strongly considered for the application as conducting additives. The one-dimensional (1D) CNTs afford ultrahigh conductivity (10^4 S cm^{-1} at 300 K for single walled CNTs and >10^3 S m^{-1} for multiwalled

Received: July 18, 2013
Revised: October 4, 2013
Published: October 27, 2013

nanotubes (MWCNTs)). The MWCNTs can be mass produced by fluidized bed chemical vapor deposition (CVD) at a very low cost (less than \$100 kg^{-1}),[24,25] and they can be well-dispersed into a solvent (e.g., *N*-methyl-2-pyrrolidone (NMP)) as CNT conductive paste. Moreover, the unique 1D structure is especially beneficial for the construction of a robust conducting network, thanks to its superior mechanical properties and large length to diameter ratio. Therefore, by mixing the metal oxide/phosphate cathodes with CNT paste and binder, 3D conductive CNT scaffolds are available to improve the Li ion storage performance.[12,26,27] The uses of graphene nanosheets as conductive fillers are also reported recently.[19−21] However, the CNTs prefer to be agglomerated into bundles and offer limited attached sites, while graphene layers tend to stack with each other due to the strong van der Waals interactions. The combination of nanocarbon building blocks into hierarchical nanostructures/hybrids is expected to bring well distribution of each elements and even lead to formation of multifunctional materials with unexpected performances.[28] Very recently, Wu et al. demonstrated that the decoration of double nanocarbon (amorphous carbon coating and graphitized conducting carbon) onto $LiFePO_4$ nanocomposite led to ultrahigh rate capability.[29] Consequently, the strategies toward fully demonstrating the potentials of nanocarbon as 3D conductive scaffolds for cathode are highly required.

In this contribution, the use of CNTs and/or CBs as conductive scaffolds of $LiFePO_4$ cathodes was explored. A 3D hierarchical CNT/CB network was fabricated to increase the conductive contacts among the nanoparticles. The Li ion storage characters of CB, CNT, and CNT/CB fillers were evaluated to demonstrate the proof-of-the-concept of synergy effects between nanocarbon conductive fillers.

MATERIALS AND METHODS

Materials for Conductive Pastes. The $LiFePO_4$ was prepared by a routine hydrothermal process similar to the previous publications.[9] A conductive carbon layer was uniformly coated on the $LiFePO_4$ particles with glucose as carbon sources.[6] The Super P conductive CBs based on partial oil oxidation of petrochemical raw materials were with a size of 20−60 nm. The CNTs with a diameter of 8−12 nm, a length of 30−100 μm, a typical length-to-diameter ratio of 10^3−10^4, Brunauer−Emmett−Teller specific surface area of ∼230 m^2 g^{-1}, and agglomerated morphology were mass produced by fluidized bed CVD.[24] The conductive additives were ball milled for 2 h and dispersed into NMP with a concentration of 5 wt % as conductive pastes. CB/CNT mixture with a ratio of 1:2 and raw CBs were also prepared as conductive paste to construct composite cathodes for Li-ion battery.

Characterizations. The morphology of the electrode was characterized using a JSM 7401F scanning electron microscope (SEM) operated at 3.0 kV, and a JEM 2010 high resolution transmission electron microscope (TEM) operated at 120.0 kV.

Li Storage Performance Evaluation. To compare the performances of various conductive additives, the working cathodes were prepared through a slurry route. A slurry was first available by mixing the $LiFePO_4$/C active material, conductive additive (CNTs, CBs, or CNT/CB mixture), and polyvinylidene fluoride (PVDF) in NMP binder with a weight ratio of $LiFePO_4$/C:conductive additive:PVDF binder = 90:5:5 (for cycling test) or 85:10:5 for (for rate test). To prepare homogeneously mixed slurry, vigorously magnetic stirring was carried out for ca. 24 h. The as-obtained slurry was later uniformly coated onto an Al foil and, then, dried in a vacuum drying oven at 120 °C for 12 h. The foil was punched into disks with a diameter of 13 mm for the working electrode. The electrochemical testing was carried out by coin cells of CR2025 with a Li foil as the anode, a microporous polyethylene sheet (Celgard 2400) as the separator, and $LiPF_6$ (1.0 mol L^{-1}) as the electrolyte which was dissolved in a mixed solution of dimethyl carbonate (DMC), ethylene carbonate (EC), and ethylene methyl carbonate (EMC) (mass ratio of DMC:EC:EMC = 1:1:1). All the assembly processes for the coin cells were conducted in an argon-filled glovebox. To ensure the comparability of the results, the capacity of the material was calculated based on the mass of $LiFePO_4$/C active material. The cells were charged and discharged over a voltage range of 2.5−4.0 V at different currents using Neware multichannel battery cycler. The cyclic voltammetry (CV) were carried out on a Solartron Analytical 1470E electrochemical workstation at a sweep rate of 0.1 mV s^{-1} between 2.5 and 4.0 V (vs Li/Li^+). The electrochemical impedance spectroscopy (EIS) was also collected on the Solartron Analytical 1470E electrochemical workstation. The impedance spectra were measured with Li-metal as the counter electrode at various voltages (2.5−4.0 V) during the first charge−discharge cycle.

RESULTS AND DISCUSSION

Morphology of Composite Cathode with Different Conductive Additives. The morphologies of composite cathode with CBs as conductive agents were shown in Figure 1. The average grain size of the $LiFePO_4$ was around 100−300 nm in width and 200−900 in length (Figure 1a−c). A conductive carbon layer was uniformly coated on the well-crystallized $LiFePO_4$ (Figure 1d), in which the *d*-spacing of 0.372 nm corresponded to the (011) facet of olivine-type $LiFePO_4$, indicating the prominent crystal orientation along the *bc* plane. CBs were one of the most common conductive additives in lithium ion battery industry. However, the small-diameter particles tended to aggregate and could not perfectly attach to $LiFePO_4$ particles (Figure 1b and c). This behavior reduced the efficiency in constructing conducting networks for CB conducting additives, especially at a reduced amount of conductive additives of only 5 wt %. Consequently, CBs could not form a robust and interconnected conductive scaffold at a low loading amount.

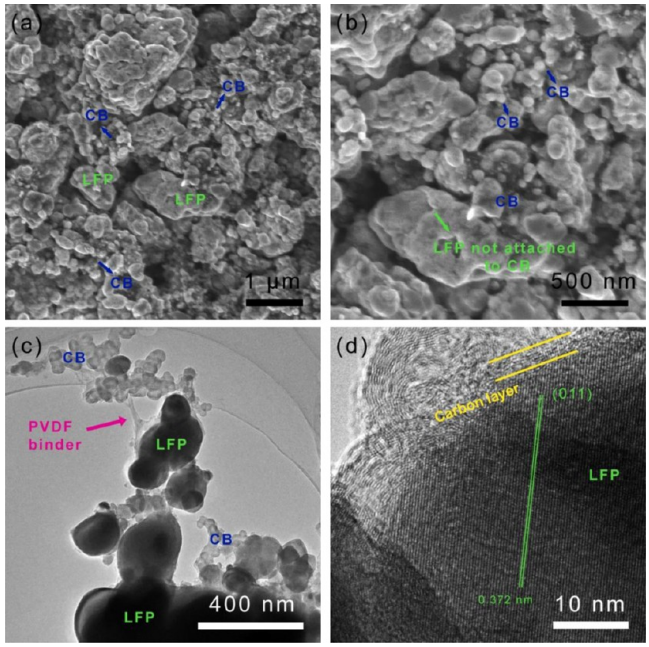

Figure 1. (a and b) SEM images of composite cathode consisted of $LiFePO_4$/C and CB. (c and d) TEM images of composite cathode consisted of $LiFePO_4$/C and CB. The $LiFePO_4$ was abbreviated as LFP.

When using CNTs as conductive additives (Figure 2), a 3D conductive network was formed by the interconnected CNTs

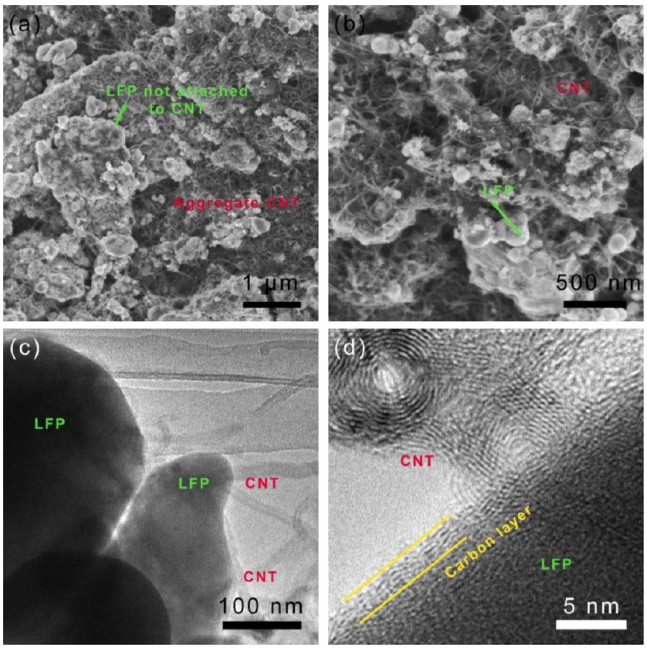

Figure 2. (a and b) SEM images of composite cathode consisted of $LiFePO_4$/C and CNTs. (c and d) TEM images of composite cathode consisted of $LiFePO_4$/C and CNTs.

around $LiFePO_4$ particles. Most of $LiFePO_4$ particles were embedded into the CNT network and attached with each other (Figure 2b). When Li^+ inserted into/extracted from the stable olivine-type crystalline during the electrochemical reaction, the electron efficiently transferred through CNT network to the coated carbon layers and $LiFePO_4$ active phases if effective physical contact between CNTs and $LiFePO_4$/C particles were available (Figure 2c and d). However, CNTs tended to agglomerate with each other in some cases (Figure 2a) and therefore impaired the full utilization of this materials in forming high efficient conductive networks. As a result, the electrical performance of the cathode is still limited.

With the coupling of conductive CBs addition and CNTs (Figure 3), both the CBs and CNTs were employed as electron pathways. A 3D long-range conductive network was constructed by CNTs as scaffold and CBs as paste. Attributed from their spherical morphology, CBs were mainly distributed in the gap among $LiFePO_4$/C particles or $LiFePO_4$/C and CNTs (Figure 3a and b). As confirmed by the TEM image (Figure 3c and d), the CB particles were well attached with the carbon layers on the $LiFePO_4$ particles. The π electrons vertical to the sp^2 plane were assumed to be well shared among carbon layers on the $LiFePO_4$ particles, CBs, and CNTs, obtaining a stable and continuous system for electron transportation. Therefore, even the amount of CNTs decreased greatly, the long-range conductive network was well maintained.

Meanwhile, the short-range conductive pathways among $LiFePO_4$/C particles as well as among $LiFePO_4$/C and CNTs were well built by CB pastes. Such a hierarchical conductive network could make full use of the electrochemical potential of $LiFePO_4$ when a rather limited amount of conductive addition was employed to accommodate the commercial demand of Li-ion battery industry.

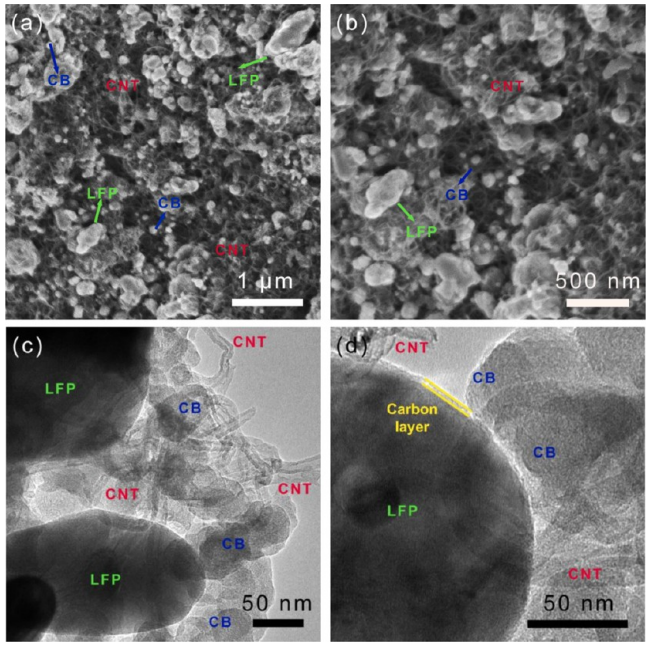

Figure 3. (a and b) SEM images and (c and d) TEM images of CNT/CB modified $LiFePO_4$/C cathodes.

Li Storage Performance on CNT(CB)/$LiFePO_4$ Cathodes. The electrochemical properties of composite cathodes were evaluated with 2025-type coin half-cells to demonstrate the performance of the conductive agents for their potential applications in Li-ion batteries. The CV profiles were performed with the operation voltage in the range of 2.5−4.0 V vs Li/Li^+. Figure 4 showed a typical first three cycles of the

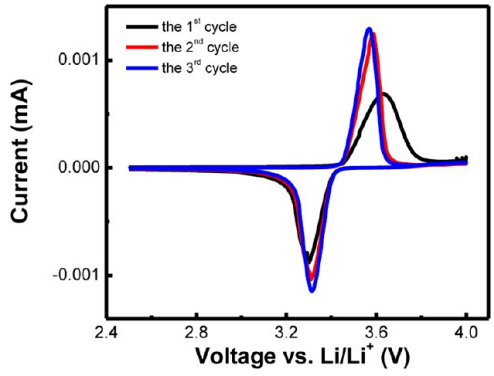

Figure 4. Typical CV curves on $LiFePO_4$/C cathode with CNT/CB additives.

CV profiles of $LiFePO_4$/C cathodes with CNT/CB additives at a scanning rate of 0.1 mV s^{-1}. The electrodes exhibited a couple of anodic and cathodic peaks in the range of 3.30−3.63 V, corresponding to the two-phase charge/discharge reaction between $LiFePO_4$ and $FePO_4$. The position of redox peaks corresponded to the extraction and insertion of Li^+. During the first cycle, the anodic peak was at 3.63 V, while the corresponding cathodic peak was at 3.30 V. In the second and third cycles, the anodic peak was at 3.58 V, and the corresponding cathodic peak was nearly unaltered. The use of CNT/CB network offered a good conductive network with approximately symmetrical peaks and few polarization of cathode during anodic/cathodic scan, indicating the excellent

dx.doi.org/10.1021/sc400239u | ACS Sustainable Chem. Eng. 2014, 2, 200−206

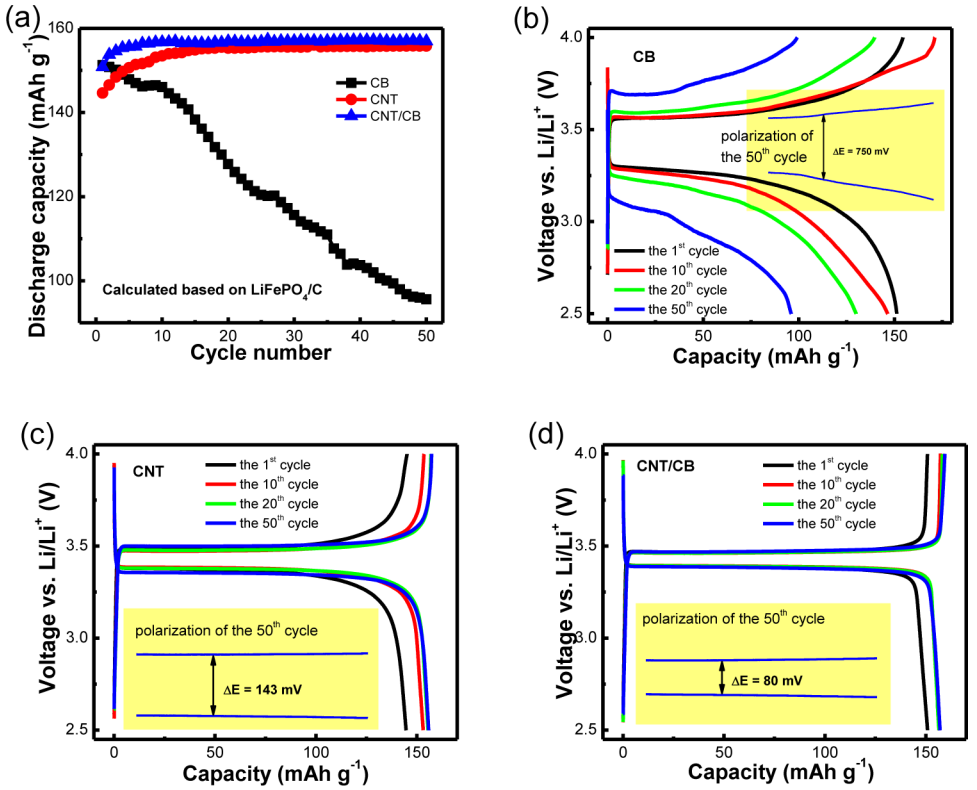

Figure 5. (a) Discharge capacity vs cycle number for the $LiFePO_4$/C cathode with CBs, CNTs, and CNTs/CBs as conductive scaffolds. The voltage profile for the galvanostatic charge−discharge curves of the $LiFePO_4$/C cathode with (b) CBs, (c) CNTs, and (d) CNTs/CBs as conductive scaffolds, and corresponding polarization value of the 50th cycle (inset figure).

insertion/extraction reversibility. This was similar to those of CBs[4] or CNTs[6] as the conductive fillers but exhibited less polarization.

The cycling performances of $LiFePO_4$/C composite cathodes with CBs, CNTs, and CNTs/CBs as conductive networks were investigated at a current density of 0.2 C (a current density of 170 mA g^{-1} (1 C) equivalent to fully discharge or charge in 1 h was applied in both current sweep directions) (Figure 5). Although the cathode with conductive network consisting of only CB-units exhibited a high initial discharge capacity of 151.2 mAh g^{-1}, the polarization became obviously worse as the cycling number increased, leading to a significant capacity loss. After 50 cycles, the capacity was 95.6 mAh g^{-1} with a capacity retention of only 63.2%. The galvanostatic charge−discharge curves suffered huge distortion, and the potential plateaus around 3.41 V (vs Li/Li^+), which can be associated to the Fe^{3+}/Fe^{2+} redox couple, disappeared gradually (Figure 5b). The capacity decay and the severe polarization suggested that conductive network consist of CB spheres failed to maintain a well-contacting status and continuous electron pathway during charge−discharge process. The test cells with CNTs as conductive fillers displayed a better cycling performance with low polarization. An initial discharge capacity of 144.6 mAh g^{-1} was available, while after electrolyte penetration, the capacity of the 50th cycle increased to 155.8 mAh g^{-1}, which was enormously better than cells with only CBs. Such improvement in both discharge capacity and stability is attributed to the excellent intrinsic electrical conductivity along the *c*-axis of CNTs as well as the robust and continuous 3D framework consisting of interlaced 1D nanotubes. However, with the partial replacement of CNTs into CBs, the cycling performance was dramatically improved. For instance, an initial discharge capacity of 150.8 mAh g^{-1} and a 50th-cyclic capacity of 156.9 mAh g^{-1} were demonstrated on composite cathode with CNT/CB hierarchical conductive networks. The polarization value ΔE evaluated from the difference between the voltage of charge/discharge potential plateaus at the 50th cycle was 750, 143, and 80 mV for CB, CNT, and CNT/CB modified composite cathode, respectively (Figure 5b−d), which indicated the progressively improved electrochemical kinetics of CNT and CNT/CB hierarchical scaffolds.

Such hierarchical CNT/CB networks exhibited even more prominent advantages at higher charge−discharge rate. The rate performance of the sample was shown as Figure 6. When used only CBs, the as-obtained cathode delivered almost no capacity under large current (such as 0.8 C). In contrast, the

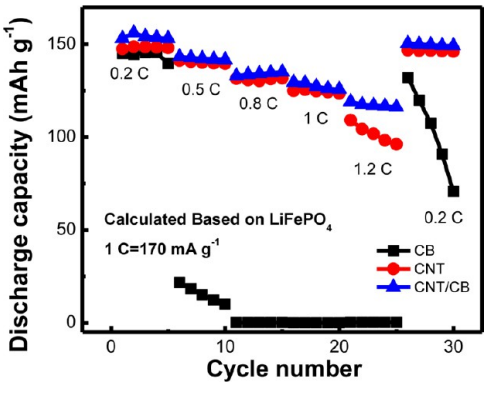

Figure 6. Rate performance (discharge capacity) of the $LiFePO_4$/C cathode with CBs, CNTs, and CNTs/CBs as conductive networks.

dx.doi.org/10.1021/sc400239u | ACS Sustainable Chem. Eng. 2014, 2, 200−206

$LiFePO_4$/C cathode with CNTs as conductive agent exhibited a reversible discharge capacity of 148.6 and 109.0 mAh g^{-1} at a charge−discharge current density of 0.2 and 1.2 C, respectively. When the CBs as well as CNTs were introduced simultaneously, the discharge capacity increased obviously due to the hierarchical architecture and synergistic effect of CNTs and CBs. A discharge capacity of 156.1 mAh g^{-1} at a charge−discharge current density of 0.2 C were demonstrated on CNT/CB modified $LiFePO_4$/C cathode, while at 1.2 C, a capacity of 119.1 mAh g^{-1} was still preserved, indicating an outstandingly improved rate performance even with very little conductive agents. The combination of CNTs and CBs ensured high electron-transfer efficiency at different scales and interfaces during the rapid charge−discharge process. Furthermore, the electrical performances can be further enhanced by tuning the ratio of CNTs to CBs. When the current density decreased from 1.2 to 0.2 C, the discharge capacity recovered back, indicating good reversibility at high current density, which strongly benefited from the stable hierarchical conductive network.

The EIS was used to evaluate electrode impedance of the composite cathodes. The fitting equivalent circuit,[6,30] in which the resistance (R), constant phase element (CPE), and Warburg impedance element (W) were included, was shown as the inset illustration of Figure 7. R_s was associated with the

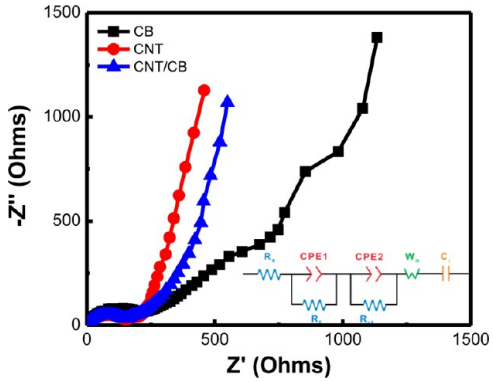

Figure 7. Electrochemical impedance spectra of the $LiFePO_4$/C cathode with CB, CNT, and CNT/CB as conductive networks.

solution resistance of electrolyte and other cell components; R_f and CPE1 were related to the solid-state diffusion of Li^+ through the solid electrolyte interface and its corresponding CPE, respectively; R_{ct} and CPE2 signified the charge transfer resistance and the corresponding CPE, respectively; W_o was the Warburg impedance element attributable to the diffusion of lithium ions in the active materials; C_i was an intercalation capacitance. The fitting results were listed in Table 1. The resistance values of composite cathodes during the charge−discharge cycles showed a similar trend. However, the $R_{(ct+f)}$ value of $LiFePO_4$/C with CNT/CB hierarchical conductive scaffold was smaller than those of the cathodes with the other two fillers. Such fitting results provided an unambiguous evidence for the easy and rapid Li ion diffusion and good electron transfer pathway, as well as the improved conductive interfacial effect on the hybrid conductive additives. Such improved kinetics on the $LiFePO_4$/C electrode are attributed to the advantages of the hierarchical conductive framework in multidimension from the excellent attachment to active materials into the long-range conducting network, which were well confirmed by the SEM and TEM images (Figure 1−3).

Proposed Mechanism of Hierarchical CNT/CB Conductive Network with Enhanced Li Storage Performance. The proposed model to describe the use of CB, CNT, and CB/CNT scaffolds as efficient electron pathways is illustrated as Figure 8. Due to their spherical morphology,

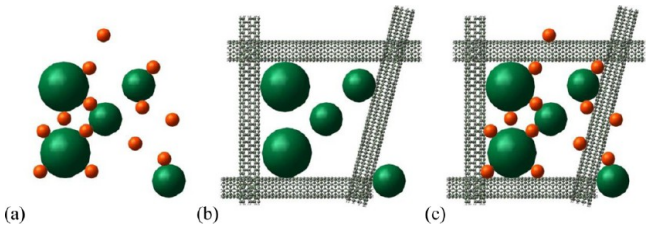

Figure 8. Schematic of (a) CB (red spheres), (b) CNT (gray tubules), and (c) hierarchical CB/CNT network as conductive additive for $LiFePO_4$/C (green spheres) composite cathodes.

small size around 20−60 nm, and considerably high conductivity, CBs, on one hand, provide abundant contacting sites with $LiFePO_4$/C particles and are more capable of building short-range electron pathway through surface adhesions and interactions; on the other hand, attributed from the zero-dimensional limitation from their small featured size, CBs tend to aggregate or localize on the surface of active material particles instead of assembling into long-chain bead-like conductive pathways to form continuous scaffolds (Figure 8a). Even if CBs are constructed into an interconnected network initially, the weak physical connections between individual CB particles render low mechanical strength and poor structural stability, leading to the fast degradation of conducting network and therefore short lifetime (as shown in Figure 5a).

Well-dispersed CNTs are adequate in building long-range conducting scaffolds because of their unique 1D tubular morphology and outstanding electrical and mechanical properties along *c*-axis. On one hand, electron migrates very rapidly along the *c*-axis of CNTs without transmitting through too many interfaces as in CB network; on the other hand, the network consisting of interlaced CNTs is robust enough, resulting in high capacity retention. However, the 1D nanotubes limit the number of contacting sites with $LiFePO_4$/C particles. The rapid electron-transfer also suffers oriental limitations which differ from *c*-axis and the perpendicular direction to the surfaces of CNTs. Those limitations render low electron-transfer efficiency of CNTs at a short-range scale, and even some $LiFePO_4$/C particles are not

Table 1. Fitting Results of EIS of Cathodes with Various Types of Conducting Fillers

fillers	R_s (Ω)	CPE1 (μF)	R_f (Ω)	CPE2 (μF)	R_{ct} (Ω)	$R_{(f+ct)}$ (Ω)	W_o (Ω $s^{0.5}$)	C_i (mF)
CB	1.29	6.85	165.9	3.15	28.98	194.9	0.0021	0.00
CNT	3.66	2.01	34.72	7.67	112.3	147.0	0.0080	22.65
CNT/CB	1.61	6.87	112.9	2.41	26.02	138.9	0.0049	46.79

dx.doi.org/10.1021/sc400239u | ACS Sustainable Chem. Eng. 2014, 2, 200−206

attached to the CNT conductive network, which are incapable of capacity contribution (Figure 8b).

The cathodes with hybridized CBs and CNTs forming hierarchical scaffolds possess both short- and long-range electron pathways, which provide both a surface conductive layer with abundant contacting sites to $LiFePO_4$/C particles and interconnected and continuous 3D networks (Figure 8c). The hybridized point-to-point and line-to-point contact of CBs, CNTs, and $LiFePO_4$/C particles provides the effective electron pathway. It is reported that the CBs are tightly attached on the side walls of CNTs/graphene, which have a positive role in the dispersion of CNTs/graphene.[31,32] Herein, an interconnected π-conjugated environment is well-built among carbon layers on the $LiFePO_4$ particles, CBs, and CNTs in this hierarchical conductive scaffold. Consequently, CBs and CNTs synergistically promote the efficiency of electron transfer at different scales. Such structure design is consistent to its outstanding Li storage performances and also is scalable and easy to extend to composite cathode design of other Li-ion battery cathode material for various commercial applications. For example, two-dimensional (2D) graphene is a promising candidate as conductive additives for electrochemical energy storage application.[10] However, mass production of high-quality and unstacked 2D graphene nanosheets via facile, environmentally friendly, and efficient method still need to be explored, which limits its commercial application. The hybridization of 2D graphene and zero dimensional CB is a potential approach for enhanced electrochemical performance and reduced cost. By partially replacing the relatively costly CNTs/graphene with other inexpensive conductive additives such as CBs, the as-obtained composite cathodes demonstrate excellent electrical performances as well as less addition of conductive fillers.[33] Such a strategy is well applied not only in Li ion battery, but also in super capacitors, Li/S batteries, as well as Li/O_2 batteries which required robust and high conductive scaffolds.[1,34,35]

CONCLUSIONS

A hierarchical 3D scaffold consisting of CNTs and CBs was employed as conductive fillers in the cathode of Li-ion batteries. The as-obtained composite cathodes with hybridized CBs and CNTs possessed both short- and long-range electron pathways, which provided both a surface conductive layer with abundant contacting sites to $LiFePO_4$/C particles and interconnected continuous 3D networks. Therefore, the $LiFePO_4$/C cathode showed enhanced Li storage performance and ameliorative electrochemical kinetics. The $LiFePO_4$/C cathode with such hierarchical CNTs/CBs network exhibited reversible discharge capacity of 156.9 mAh g^{-1} over 50 cycles at a current density of 0.2 C. When current density increased to 1.2 C, a capacity of 119.1 mAh g^{-1} was preserved, and a capacity of 150.5 mAh g^{-1} at 0.2 C rate was available after 1.2 C rate, indicating a high reversibility of the composite cathode. This strategy to hybridize CNTs and CBs into a hierarchical 3D network has demonstrated its high efficiency to build $LiFePO_4$/C composite cathode with excellent Li storage performance and good economy. Such design can be easily extended to various cathode materials for Li-ion batteries, as well as super capacitors, redox flow batteries, and Li/S as well as Li/O_2 batteries with extraordinary energy storage performance.

AUTHOR INFORMATION

Corresponding Author

*E-mail: zhang-qiang@mails.tsinghua.edu.cn.

Author Contributions

$^{\perp}$X.-Y.L. and H.-J.P.: These authors contributed equally.

Notes

The authors declare no competing financial interest.

ACKNOWLEDGMENTS

This work was supported by the National Basic Research Program of China (973 Program, 2011CB932602 and 2011CB935902).

REFERENCES

(1) Su, D. S.; Schlogl, R. Nanostructured Carbon and Carbon Nanocomposites for Electrochemical Energy Storage Applications. *ChemSusChem* **2010**, *3*, 136−168.

(2) Yuan, L. X.; Wang, Z. H.; Zhang, W. X.; Hu, X. L.; Chen, J. T.; Huang, Y. H.; Goodenough, J. B. Development and Challenges of $LiFePO_4$ Cathode Material for Lithium-Ion Batteries. *Energy Environ. Sci.* **2011**, *4*, 269−284.

(3) Wu, C. Y.; Cao, G. S.; Yu, H. M.; Xie, J.; Zhao, X. B. In Situ Synthesis of $LiFePO_4$/Carbon Fiber Composite by Chemical Vapor Deposition with Improved Electrochemical Performance. *J. Phys. Chem. C* **2011**, *115*, 23090−23095.

(4) Reddy, M. V.; Subba Rao, G. V.; Chowdari, B. V. R. Metal Oxides and Oxysalts as Anode Materials for Li Ion Batteries. *Chem. Rev.* **2013**, *113*, 5364−5457.

(5) Dominko, R.; Bele, M.; Gaberscek, M.; Remskar, M.; Hanzel, D.; Pejovnik, S.; Jamnik, J. Impact of the Carbon Coating Thickness on the Electrochemical Performance of $LiFePO_4$/C Composites. *J. Electrochem. Soc.* **2005**, *152*, A607−A610.

(6) Liu, X. F.; Huang, J. Q.; Zhang, Q.; Liu, X. Y.; Peng, H. J.; Zhu, W. C.; Wei, F. N-Methyl-2-Pyrrolidone-Assisted Solvothermal Synthesis of Nanosize Orthorhombic Lithium Iron Phosphate with Improved Li-Storage Performance. *J. Mater. Chem.* **2012**, *22*, 18908−18914.

(7) Inagaki, M. Carbon Coating for Enhancing the Functionalities of Materials. *Carbon* **2012**, *50*, 3247−3266.

(8) Chung, S. Y.; Bloking, J. T.; Chiang, Y. M. Electronically Conductive Phospho-Olivines as Lithium Storage Electrodes. *Nat. Mater.* **2002**, *1*, 123−128.

(9) Wang, L.; He, X. M.; Sun, W. T.; Wang, J. L.; Li, Y. D.; Fan, S. S. Crystal Orientation Tuning of $LiFePO_4$ Nanoplates for High Rate Lithium Battery Cathode Materials. *Nano Lett.* **2012**, *12*, 5632−5636.

(10) Kang, F. Y.; Ma, J.; Li, B. H. Effects of Carbonaceous Materials on the Physical and Electrochemical Performance of a $LiFePO_4$ Cathode for Lithium-Ion Batteries. *New Carbon Mater.* **2011**, *26*, 161−170.

(11) Dominko, R.; Gaberscek, M.; Drofenik, J.; Bele, M.; Pejovnik, S.; Jamnik, J. The Role of Carbon Black Distribution in Cathodes for Li Ion Batteries. *J. Power Sources* **2003**, *119*, 770−773.

(12) Li, X. L.; Kang, F. Y.; Bai, X. D.; Shen, W. A Novel Network Composite Cathode of $LiFePO_4$/Multi-walled Carbon Nanotubes with High Rate Capability for Lithium Ion Batteries. *Electrochem. Commun.* **2007**, *9*, 663−666.

(13) Jin, B.; Gu, H. B.; Zhang, W. X.; Park, K. H.; Sun, G. P. Effect of Different Carbon Conductive Additives on Electrochemical Properties of $LiFePO_4$-C/Li Batteries. *J. Solid State Electr.* **2008**, *12*, 1549−1554.

(14) Jin, B.; Jin, E. M.; Park, K. H.; Gu, H. B. Electrochemical Properties of $LiFePO_4$-Multiwalled Carbon Nanotubes Composite Cathode Materials for Lithium Polymer Battery. *Electrochem. Commun.* **2008**, *10*, 1537−1540.

(15) Liu, Y. J.; Li, X. H.; Guo, H. J.; Wang, Z. X.; Peng, W. J.; Yang, Y.; Liang, R. F. Effect of Carbon Nanotube on the Electrochemical Performance of C- $LiFePO_4$/Graphite Battery. *J. Power Sources* **2008**, *184*, 522−526.

(16) Chen, M.; Du, C. Y.; Song, B.; Xiong, K.; Yin, G. P.; Zuo, P. J.; Cheng, X. Q. High-Performance $LiFePO_4$ Cathode Material from $FePO_4$ Microspheres with Carbon Nanotube Networks Embedded for Lithium Ion Batteries. *J. Power Sources* **2013**, *223*, 100−106.
(17) Wang, G. P.; Li, H.; Zhang, Q. T.; Yu, Z. L.; Qu, M. Z. The Study of Carbon Nanotubes as Conductive Additives of Cathode in Lithium Ion Batteries. *J. Solid State Electr.* **2011**, *15*, 759−764.
(18) Endo, M.; Kim, Y. A.; Hayashi, T.; Nishimura, K.; Matusita, T.; Miyashita, K.; Dresselhaus, M. S. Vapor-Grown Carbon Fibers (VGCFs) - Basic Properties and Their Battery Applications. *Carbon* **2001**, *39*, 1287−1297.
(19) Su, F. Y.; You, C. H.; He, Y. B.; Lv, W.; Cui, W.; Jin, F. M.; Li, B. H.; Yang, Q. H.; Kang, F. Y. Flexible and Planar Graphene Conductive Additives for Lithium-Ion Batteries. *J. Mater. Chem.* **2010**, *20*, 9644−9650.
(20) Kim, H.; Kim, H.; Kim, S. W.; Park, K. Y.; Kim, J.; Jeon, S.; Kang, K. Nano-Graphite Platelet Loaded with $LiFePO_4$ Nanoparticles Used as the Cathode in a High Performance Li-Ion Battery. *Carbon* **2012**, *50*, 1966−1971.
(21) Yang, J. L.; Wang, J. J.; Tang, Y. J.; Wang, D. N.; Li, X. F.; Hu, Y. H.; Li, R. Y.; Liang, G. X.; Sham, T. K.; Sun, X. L. $LiFePO_4$-Graphene as a Superior Cathode Material for Rechargeable Lithium Batteries: Impact of Stacked Graphene and Unfolded Graphene. *Energy Environ. Sci.* **2013**, *6*, 1521−1528.
(22) Zhao, M. Q.; Liu, X. F.; Zhang, Q.; Tian, G. L.; Huang, J. Q.; Zhu, W. C.; Wei, F. Graphene/Single-Walled Carbon Nanotube Hybrids: One-Step Catalytic Growth and Applications for High-Rate Li-S Batteries. *ACS Nano* **2012**, *6*, 10759−10769.
(23) Chen, S. Q.; Bao, P.; Wan, G. X. Synthesis of Fe_2O_3-CNT-Graphene Hybrid Materials with an Open Three-Dimensional Nanostructure for High Capacity Lithium Storage. *Nano Energy* **2013**, *2*, 425−434.
(24) Zhang, Q.; Huang, J. Q.; Zhao, M. Q.; Qian, W. Z.; Wei, F. Carbon Nanotube Mass Production: Principles and Processes. *ChemSusChem* **2011**, *4*, 864−889.
(25) Zhang, Q.; Huang, J. Q.; Qian, W. Z.; Zhang, Y. Y.; Wei, F. The Road for Nanomaterials Industry: A Review of Carbon Nanotube Production, Post-Treatment, and Bulk Applications for Composites and Energy Storage. *Small* **2013**, *9*, 1237−1265.
(26) Zhang, Q. T.; Qu, M. Z.; Niu, H.; Yu, Z. L. A Nanocarbon Composite as a Conducting Agent to Improve the Electrochemical Performance of a $LiCoO_2$ Cathode. *New Carbon Mater.* **2007**, *22*, 361−364.
(27) Wang, K.; Wu, Y.; Luo, S.; He, X. F.; Wang, J. P.; Jiang, K. L.; Fan, S. S. Hybrid Super-Aligned Carbon Nanotube/Carbon Black Conductive Networks: A Strategy to Improve Both Electrical Conductivity and Capacity for Lithium Ion Batteries. *J. Power Sources* **2013**, *233*, 209−215.
(28) Zhao, M. Q.; Zhang, Q.; Huang, J. Q.; Wei, F. Hierarchical Nanocomposites Derived from Nanocarbons and Layered Double Hydroxides - Properties, Synthesis, and Applications. *Adv. Funct. Mater.* **2012**, *22*, 675−694.
(29) Wu, X.-L.; Guo, Y.-G.; Su, J.; Xiong, J.-W.; Zhang, Y.-L.; Wan, L.-J. Carbon-Nanotube-Decorated Nano-$LiFePO_4$@C Cathode Material with Superior High-Rate and Low-Temperature Performances for Lithium-Ion Batteries. *Adv. Energy Mater.* **2013**, *3*, 1155−1160.
(30) Reddy, M. V.; Rao, G. V. S.; Chowdari, B. V. R. Long-Term Cycling Studies on 4V-Cathode, Lithium Vanadium Fluorophosphate. *J. Power Sources* **2010**, *195*, 5768−5774.
(31) Liu, W. B.; Pei, S. F.; Du, J. H.; Liu, B. L.; Gao, L. B.; Su, Y.; Liu, C.; Cheng, H. M. Additive-Free Dispersion of Single-Walled Carbon Nanotubes and Its Application for Transparent Conductive Films. *Adv. Funct. Mater.* **2011**, *21*, 2330−2337.
(32) Yan, J.; Wei, T.; Shao, B.; Ma, F. Q.; Fan, Z. J.; Zhang, M. L.; Zheng, C.; Shang, Y. C.; Qian, W. Z.; Wei, F. Electrochemical Properties of Graphene Nanosheet/Carbon Black Composites as Electrodes for Supercapacitors. *Carbon* **2010**, *48*, 1731−1737.
(33) Su, F. Y.; He, Y. B.; Li, B. H.; Chen, X. C.; You, C. H.; Wei, W.; Lv, W.; Yang, Q. H.; Kang, F. Y. Could Graphene Construct an Effective Conducting Network in a High-Power Lithium Ion Battery? *Nano Energy* **2012**, *1*, 429−439.
(34) Huang, J. Q.; Liu, X. F.; Zhang, Q.; Chen, C. M.; Zhao, M. Q.; Zhang, S. M.; Zhu, W. C.; Qian, W. Z.; Wei, F. Entrapment of Sulfur in Hierarchical Porous Graphene for Lithium-Sulfur Batteries with High Rate Performance from-40 to 60 °C. *Nano Energy* **2013**, *2*, 314−321.
(35) Wang, D. W.; Zeng, Q. C.; Zhou, G. M.; Yin, L. C.; Li, F.; Cheng, H. M.; Gentle, I.; Lu, G. Q. Carbon/Sulfur Composites for Li-S Batteries: Status and Prospects. *J. Mater. Chem. A* **2013**, *1*, 9382−9394.